

Ni-carbon nanotubes nanocomposite for robust microelectromechanical systems fabrication

Li-Nuan Tsai, Yu-Ting Cheng, Wensyang Hsu, and Weileun Fang

Citation: *Journal of Vacuum Science & Technology B* **24**, 205 (2006); doi: 10.1116/1.2161222

View online: <http://dx.doi.org/10.1116/1.2161222>

View Table of Contents: <http://scitation.aip.org/content/avs/journal/jvstb/24/1?ver=pdfcov>

Published by the AVS: Science & Technology of Materials, Interfaces, and Processing

Articles you may be interested in

[Ni filled flexible multi-walled carbon nanotube–polystyrene composite films as efficient microwave absorbers](#)
Appl. Phys. Lett. **99**, 113116 (2011); 10.1063/1.3638462

[Diameter dependent strength of carbon nanotube reinforced composite](#)
Appl. Phys. Lett. **95**, 021901 (2009); 10.1063/1.3168520

[Power consumption reduction scheme of magnetic microactuation using electroplated Cu–Ni nanocomposite](#)
Appl. Phys. Lett. **90**, 244105 (2007); 10.1063/1.2748301

[Nitrogen-mediated fabrication of transition metal-carbon nanotube hybrid materials](#)
Appl. Phys. Lett. **90**, 013103 (2007); 10.1063/1.2428411

[Growth of aligned carbon nanotubes with controlled site density](#)
Appl. Phys. Lett. **80**, 4018 (2002); 10.1063/1.1482790

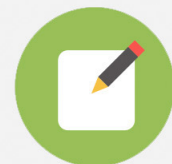


Re-register for Table of Content Alerts

Create a profile.



Sign up today!



Ni-carbon nanotubes nanocomposite for robust microelectromechanical systems fabrication

Li-Nuan Tsai

*Microsystems Integration Laboratory, Department of Electronics Engineering,
Department of Mechanical Engineering, National Chiao Tung University, 1001 Ta Hsueh Road,
Hsinchu, Taiwan, 300, Republic of China*

Yu-Ting Cheng^{a)}

*Microsystems Integration Laboratory, Department of Electronics Engineering, National Chiao Tung
University, 1001 Ta Hsueh Road, Hsinchu, Taiwan, 300, Republic of China*

Wensyang Hsu

*Department of Mechanical Engineering, National Chiao Tung University, 1001 Ta Hsueh Road, Hsinchu,
Taiwan, 300, Republic of China*

Weileun Fang

*Department of Power Mechanical Engineering, National Tsing Hua University, 1001 Ta Hsueh Road,
Hsinchu, Taiwan, 300, Republic of China*

(Received 28 July 2005; accepted 28 November 2005; published 18 January 2006)

This article presents a novel fabrication process to enhance the operational performance and reliability of electrothermal microactuators. Carbon nanotubes (CNTs) (outer diameter: 10–20 nm, inner diameter: 5–10 nm, length: 0.5–200 μm) are incorporated in an electrolytic nickel deposition process in which a well-dispersed Ni-CNTs colloidal solution is made by a special acid oxidative method to synthesis a Ni-CNTs nanocomposite for device fabrication. Measurement results show that the microactuator plated with CNTs (0.028 g/L) needs the power requirement less 95% than the pure nickel device at the same output displacement of 3 μm . The performance improvement of the electrothermal microactuator made of the nanocomposite, including device strength and power efficiency, has shown to be similar to the Ni-diamond composites (L. N. Tsai, G. R. Shen, Y. T. Cheng, and W. S. Hsu, *The 54th Electronic Components and Technology Conference*, June 2004, pp. 472–476). In addition, the E/ρ ratio of the Ni-CNTs composite can be enhanced to 1.47 times higher than that of pure nickel, which is a fascinating result for resonant device fabrication.

© 2006 American Vacuum Society. [DOI: 10.1116/1.2161222]

I. INTRODUCTION

Electrolytic (EL) plating has been a very important fabrication technique for three-dimensional microelectromechanical systems^{1,2} (MEMS) due to a variety of attractive characteristics, such as low processing temperature, low manufacturing cost, high manufacturing throughput, and better process controllability. The plating process is a galvanic chemical reaction in which metal is coated onto the object surface by passing through an electric current. With an appropriate current input, excellent film quality and high deposition rate can be simply realized by the technique suitable for MEMS fabrication. Previously, we had successfully demonstrated electrolytic Ni/nanodiamond composite synthesis and characterizations for a microelectrothermal actuator application.³ An electrothermal microactuator made of Ni/nanodiamond composite film can reduce the power requirement by 73% from 0.924 to 0.248 W; in comparison with a pure nickel device for the same 3 μm displacement. In addition, the nanocomposite microactuator can exhibit over 3 μm reversible displacement, which is larger than the pure nickel one for only with 1.8 μm displacement. Similar per-

formance enhancement by the nanocomposite strengthening effects have been found in the case of the electroless Ni–P–carbon nanotubes (CNTs) nanocomposite system.⁴ Inasmuch as the CNTs-like diamond have interesting physical properties including high mechanical strength, novel electronic properties, and excellent thermal and chemical stability, it has been observed that the Young's modulus and hardness of the Ni–P film with the incorporation of the CNTs can increase to 665.9 and 28.9 GPa values, respectively, which are four times larger than that of the pure Ni–P one.

Since the EL nickel deposition technique would provide more advantages, including stress-free, lower process temperature, and controllable film characteristics, than the electroless nanocomposite plating process, this article will present the development of the EL technique with the addition of uniformly dispersed CNTs for fabricating electrothermal microactuators. In the mean time, because the intrinsic characteristic of the nonpolarized CNT surface makes itself curled, segregated, nonuniformly distributed in water-based solution, a special acid oxidative method has to be introduced to make a well-dispersed, colloidal Ni-CNTs plating bath unlike the previous preparation of the Ni-diamond bath. We think the EL Ni-CNT nanocomposite synthesis we developed could reveal its potential application for robust MEMS

^{a)}Electronic mail: ytcheng@mail.nctu.edu.tw

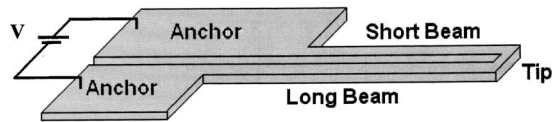


FIG. 1. Schematic diagram of the long-short-beam electrothermal microactuator.

fabrication in terms of the revealed improvement of the device performance on mechanical reliability and input power requirement in this article.

II. MICROACTUATOR DESIGN AND FABRICATION PROCESS

A. Ni-CNTs plating solution preparation

In this study, we select multiwalled CNTs for Ni-CNT nanocomposite synthesis and use the acid oxidative method⁵ to change the surface chemistry of the CNTs. The surface modification can make the nanotubes well dispersed in water-based solutions. The preparation of Ni-CNTs plating solution is the following: First, the CNTs, are put into an acidic solution of 30 mL H_2SO_4 and 20 mL H_2O_2 combination to make the carboxylate COO^- groups on the locations of the defects and the ends of the tubes. Such a treatment can effectively avoid the occurrence of the self-curl phenomenon and aggregation of the tubes in the solution. Then, the acidic solution is sonicated for 30 min to form an acidic colloidal solution. Finally, the nanocomposite plating bath is formed after mixing the colloidal solution with a commercial Ni plating solution. Because most of electrolytic Ni plating solutions function well around pH 4.0, similar neutralization of the Ni-CNTs plating solution using ammonium hydroxide² is also applied in this experiment and high-temperature distilling of CNTs solution to fully decompose residual H_2O_2 must be proceeded before being added into the nickel-plating bath because the mixture of the residual H_2O_2 and ammonium hydroxide would chemically attack the Cu seed layer, then result in disappearance.

B. Microactuator design and fabrication

The electrothermal microactuator used here is based on a long-short beam design,⁶ which consists of a pair of adjacent cantilever beams with different lengths but the same material to form an actuating arm, as shown in Fig. 1. By electrically resistive-heating two beams, the device can provide micrometer movements, which have been widely applied for electrical, optical, and biomedical instrumentations. The fabrication of the microactuator made of Ni-CNTs nanocomposite uses the same process as the previous one for the actuator made of Ni-diamond nanocomposite as shown in Fig. 2. A $2\text{ }\mu\text{m}$ high deposition pressure-chemical vapor deposition (HDP-CVD) SiO_2 is deposited as an electrical insulation and sacrificial layer, followed by a seed layer of sputtered Ti/Cu ($100\text{ }\text{\AA}/1000\text{ }\text{\AA}$) as shown in Figs. 2(a) and 2(b), respectively. Then, a $10\text{-}\mu\text{m}$ -thick photoresist is coated and patterned on top of the seed layer as the device mold of the

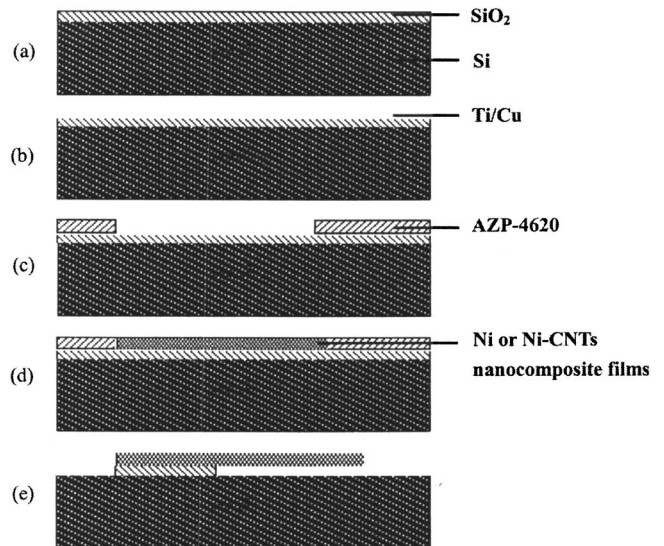


FIG. 2. Process flow of the electrothermal microactuator. (a) A $2\text{ }\mu\text{m}$ HDP-CVD SiO_2 for electrical isolation. (b) A Ti/Cu ($100\text{ }\text{\AA}/1000\text{ }\text{\AA}$) seed layer deposition. (c) A $10\text{-}\mu\text{m}$ -thick AZP-4620 coating and patterning as the plating mold. (d) Electrolytic deposition of the Ni-CNTs nanocomposite for the electrothermal microactuator. (e) Lift-off process to release the actuator.

actuator, as shown in Fig. 2(c). Finally, the wafer is put into the plating bath for a $9\text{-}\mu\text{m}$ -thick nanocomposite film deposition in which the temperature is kept at $50\text{ }^\circ\text{C}$ as shown in Fig. 2(d). Once the plating process is done, acetone, $\text{NH}_4\text{OH} + \text{H}_2\text{O}_2$, and HF solutions are used to remove the mold of PR AZP-4620, the copper seed layer, and the sacrificial layer, respectively, as shown in Fig. 2(e). Figure 3 shows an electrothermal microactuator made of the Ni-CNTs composites.

III. RESULTS AND DISCUSSIONS

For the characterization of the synthesized Ni-CNTs nanocomposites, the composite films are deposited in four different plating baths with different concentrations of CNTs, which are 0, 0.007, 0.014, and 0.028 g/L, respectively. The composition of the composite film is identified by signature

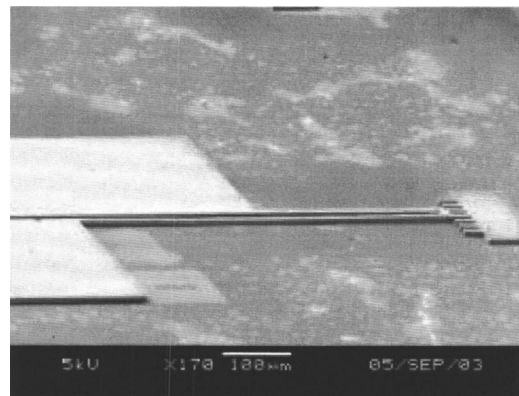


FIG. 3. Scanning electron microscopy micrograph of as-fabricated electrothermal microactuator made of the Ni-CNTs nanocomposite (Ni-0.028 g/L CNTs).

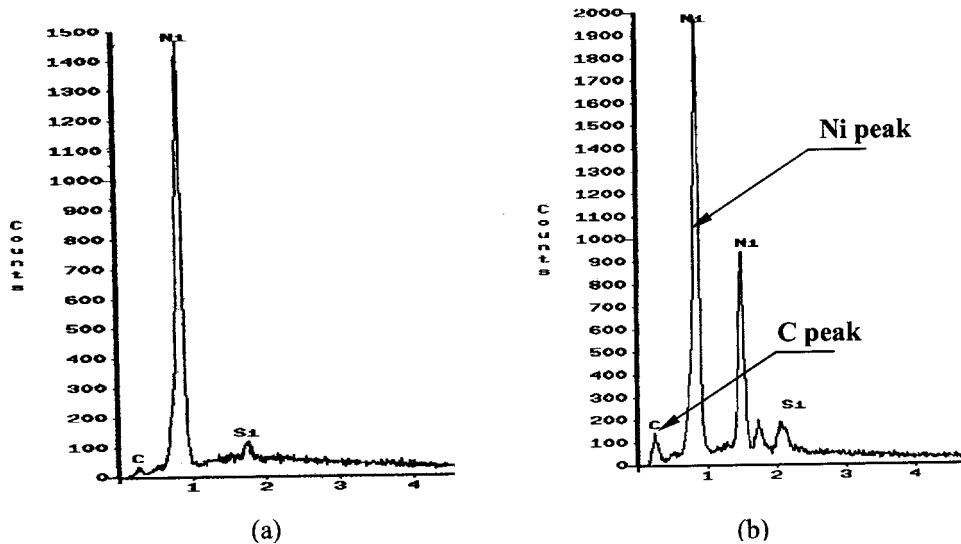


FIG. 4. EDS spectra of the pure Ni film (a) and the Ni-CNTs nanocomposite film (b).

energy-dispersive spectra (EDS). Figure 4(a) shows the EDS of a cantilever beam made of pure Ni, indicating that the electroplated layer contains very little carbon (C) in addition to Ni, Si, and O. In comparison with the EDS of the Ni-CNTs nanocomposite with larger signal intensity because of large amount of C content in the film, as shown in Fig. 4(b), the small carbon signal could be attributed to surface contamination. Figure 5 shows juxtaposed x-ray diffraction spectra of the Ni-CNTs nanocomposite and pure Ni films. The x-ray source used here is a Cu $K\alpha$ line with $\lambda = 0.154$ nm. Ni(111) and Ni (200) peaks appear at the angles of 45° and 53° , respectively, in both films, as shown in Figs. 5(a) and 5(b). However, the C (002) peak in the nanocomposite film is around $2\theta = 26^\circ$, with a 3.423 Å corresponding interlayer space that shows the existence of CNTs with trapped amorphous carbon. Similar results, which verify the real existence of the CNTs embedded in the Ni matrix, have been reported in a previous report.⁴ The surface morphology of the composite film is characterized using atomic force microscope. Figures 6 and 7 show the surface morphologies of the pure Ni and the nanocomposite films, respectively. Similar acicular appearance on the Ni-CNTs film surface is due to the incorporation of CNTs.⁷ However, the average roughness of the Ni-CNTs film is about 7.427 nm, which is comparable to that of the Ni film. It indicates the nanocomposite synthesis can still provide the same surface smoothness as pure nickel suitable for microactuator fabrication.

Regarding the mechanical characterization of the Ni-CNTs nanocomposite, the E/ρ ratio of material is used as an indicator because it is very critical to the design of the resonator for many sensor and actuator applications^{1,4,8} and can be derived from the measurement of resonant frequency of the cantilever beam made of the material. Thus, a laser doppler anemometry is used to measure the variation of resonant frequency of cantilevers made of the composites with different concentrations of the CNTs. The measured frequencies of the composites synthesized at different conditions are listed in Table I and the corresponding E/ρ values at these concentrations are plotted in Fig. 8. It is found that the E/ρ ratio

evidently increases with CNTs concentration. Furthermore, after considering the undercut effect⁹ listed in Table I, the E/ρ ratio of the Ni-CNTs nanocomposite synthesized in the plating bath with 0.028 g/L CNT particles is about 1.47

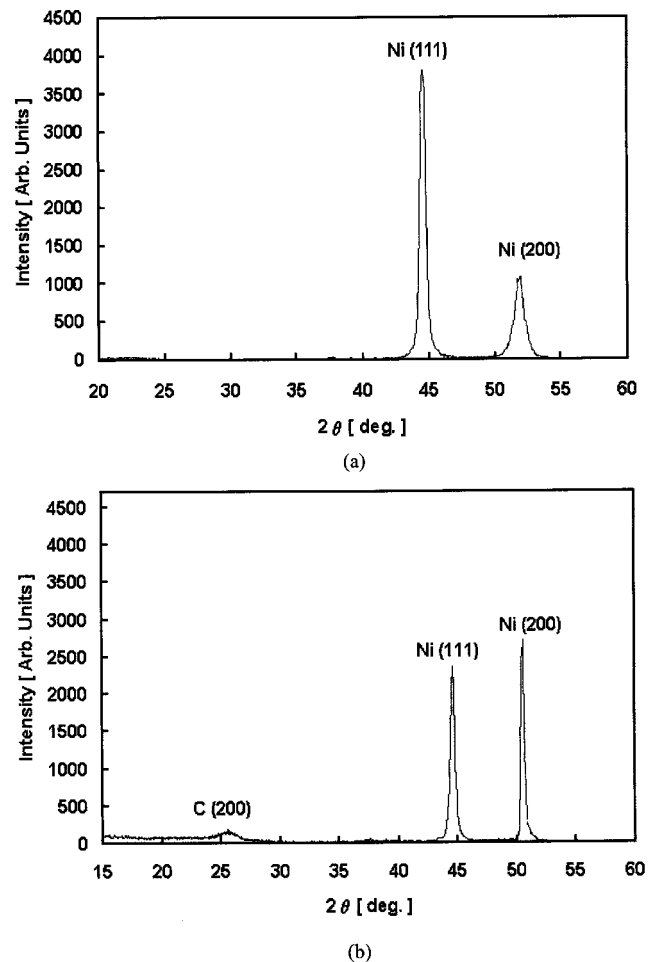


FIG. 5. X-ray diffraction spectra of the electrolytic pure Ni film (a) and the nickel-CNTs nanocomposite film (b). The carbon peak C (002) indicates the existence of CNTs.

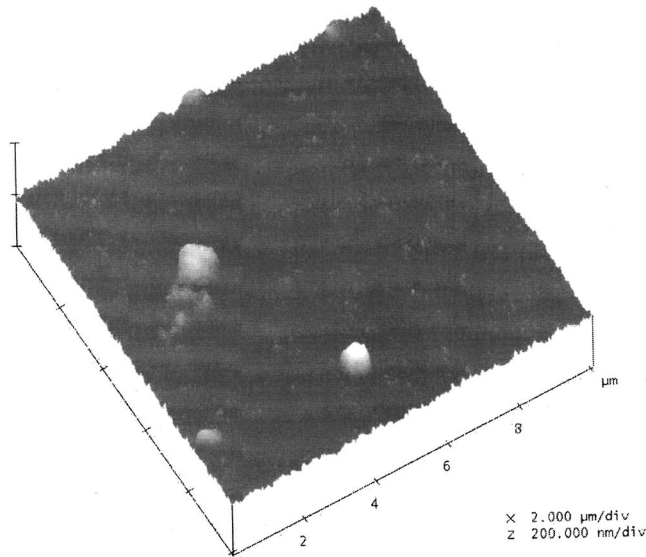


FIG. 6. Atomic force microscopy (AFM) image of the pure Ni film surface.

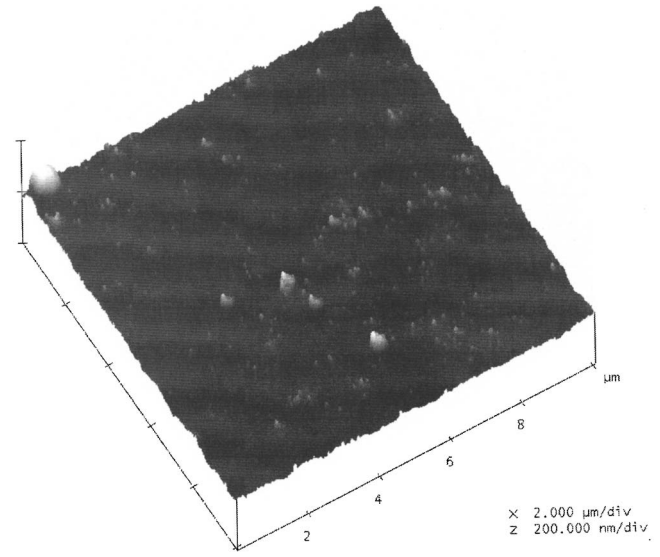


FIG. 7. AFM image of the Ni-CNTs composite film surface.

times larger than that of pure nickel, which is comparable with the enhancement achieved in the Ni/diamond nanocomposite. The correlation between the amount of the CNTs or nanodiamond incorporation and related strengthening effects still requires further investigation.

Elemental analyzer measurement is performed to correlate the synthesis process of the nanocomposites to the content of CNTs embedded in the Ni-CNTs nanocomposite film. The weight fractions of the CNTs in the Ni matrix for different plating conditions, which are 0, 0.007, 0.014, and 0.028 g/L CNTs in the baths, are 0%, 0.045%, 0.08%, and 0.085%, respectively and the corresponding volume fractions of CNTs are 0%, 8.02%, 14.26%, and 15.16%, as shown in Fig. 9. The calculation is based on the density of nickel (8.908 g/cm^3) and the bulk density of multiwalled CNT (0.05 g/cm^3) and the assumption of no existence of voids inside the films. The existence of saturation tendency in the amount of embedded CNTs in this process is found to be different from the previous electroless nanocomposite synthesis.

The electrical conductivities of the nanocomposite films are measured using the four-point probe method. Figure 10 shows that the conductivity decreases with the increase of

the incorporated CNTs concentration. Previously, Shen *et al.* has used the Maxwell-Wagner equation, as shown in Eq. (1), to estimate the electrical conductivity of the Ni-P-CNT composite film⁹

$$k_c = k_m \frac{1 + 2V_f(1 - k_m/k_d)/(1 + 2k_m/k_d)}{1 - V_f(1 - k_m/k_d)/(1 + 2k_m/k_d)}, \quad (1)$$

where V_f is the volume fraction of the second phase and k_c , k_m , and k_d are the conductivities of the composite film, matrix (Ni), and second phase (CNTs), respectively. Shen *et al.* found that the resistivity of the composite falls just within two extreme cases that are the parallel and perpendicular orientations, respectively, of the embedded CNTs to the current flow direction. However, in the Ni-CNTs composite, the conductivity k_m of a blank nickel film is $80.3 \times 10^3 \text{ s/cm}$, which is 43.4 times larger than that of the CNT. The CNT used here is a multiwalled fibrous structure with one-dimensional electrical conduction.¹⁰ The conduction only

TABLE I. Resonant frequencies of various CNTs nanoparticles concentrations in nickel matrices.

Concentration of CNTs nanoparticles (g/L)	Beam length (μm)	Effective beam length ^a (μm)	Measured resonant frequency (kHz)
0	350	188	14.031
0.007	350	30	25.504
0.014	350	24	27.826
0.028	350	20	30.42

^aThe effective beam length is equal to the original beam length minus its undercut length.

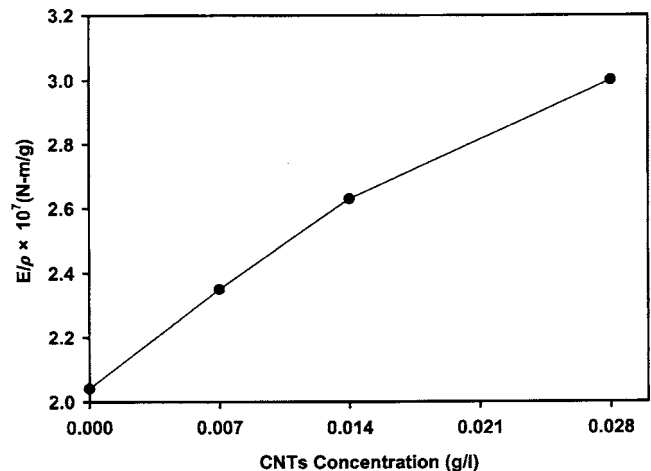


FIG. 8. E/ρ ratios of the nanocomposites plated with various CNTs concentration.

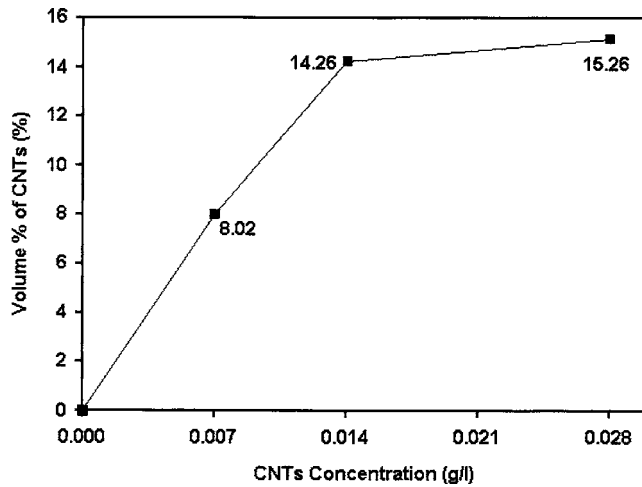


FIG. 9. Diagram of the volume fractions of the CNTs in the nanocomposite films measured by elemental analyzer.

happens along the longitudinal direction with the 1.85×10^3 s/cm conductivity (k_d). Thus, based on the assumption of the $k_m \gg k_d$ and nil conductivity contribution to the composite film for the case of the perpendicular orientation of the CNTs, the Maxwell-Wagner equation is approximated as the following:

$$k_c = k_m(1 - V_f)/(1 + V_f/2). \quad (2)$$

In comparison with measurement data as shown in Fig. 10, the simplified model provides a good estimate of the electrical conductivity of the Ni-CNTs nanocomposite.

The device performance is measured on a probe station with an automotive charge coupled device image system which can provide $0.2 \mu\text{m}$ resolution. According to the measurement data of input power versus displacement, the microactuator made of Ni-CNTs nanocomposite can have better mechanical reliability and power efficiency in comparison with that made of pure Ni film. Under the same displacement ($3 \mu\text{m}$), 0.924 W input power is required for a pure nickel

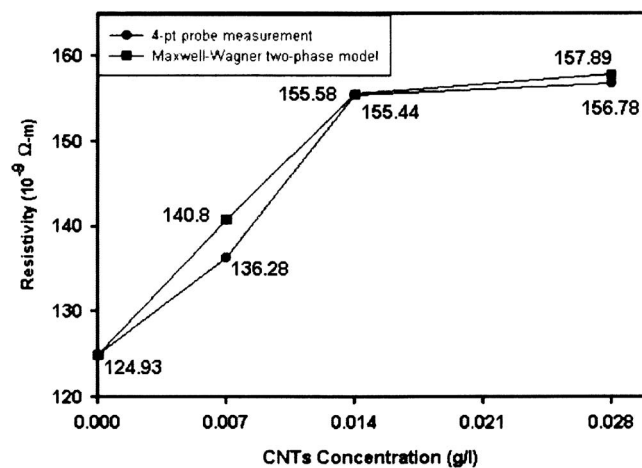


FIG. 10. Diagram of sheet resistances measured by the four-point probe and the theoretical calculations using approximated Maxwell-Wagner two-phase model.

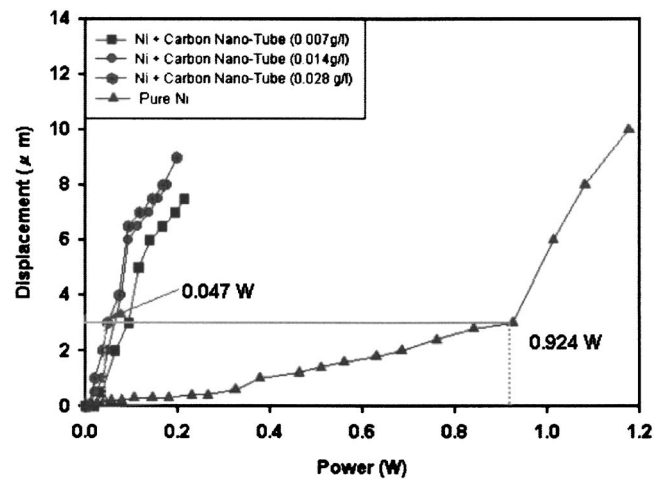


FIG. 11. Input power vs displacement of microactuators made of the nanocomposites with different CNTs concentrations.

actuator, but only 0.047 W is required for the actuator made of Ni-CNTs nanocomposite, as shown in Fig. 11. More than 95% power saving can be realized. In comparison with the pure nickel microactuator, which exhibits irreversible deformation once the output displacement is over $1.8 \mu\text{m}$, the one made of Ni-CNTs nanocomposite (0.028 g/L) can exhibit better reversible behavior only when output displacement is over $7 \mu\text{m}$. The results indicate that the Ni-CNTs microactuator can not only provide longer actuation but also more power efficient than the pure Ni one. In fact, the enhancement is similar to our previous report in the Ni/diamond nanocomposite systems, but with much larger reversible displacement.³

IV. SUMMARY

The Ni-CNT nanocomposite synthesis shows its potential application for robust MEMS fabrication. The incorporation of multiwalled carbon nanotubes (diameter: $10\text{--}20 \text{ nm}$) into the electrolytic Ni matrix can greatly enhance the mechanical properties of the Ni matrix. The characterization results show that the increase of CNTs concentration in the Ni matrix can effectively enhance the E/ρ ratio and reduce the power requirement of the electrothermal microactuator made of the composite to achieve the same output displacement as the one made of pure Ni. In addition, the Ni-CNTs nanocomposite actuator exhibits a larger reversible deformation as long as the output displacement is less than $7 \mu\text{m}$.

ACKNOWLEDGMENTS

This work is supported by the National Science Council (Taiwan) under Grant Nos. NSC 93-2220-E-009-002 and NSC 92-2212-E-009-035, and in part by MediaTek Research Center at National Chiao Tung University. The authors also would like to express their appreciation to the Nano Facility

Center of National Chiao Tung University for providing technical support and measurement facilities.

This paper was presented at the First International Workshop on One Dimensional Materials, January 10–14, 2005, National Taiwan University, Taipei, Taiwan.

¹Y. Nakamura, S. Buchailot, and L. Fujita, MEMS '97, Proceedings, *IEEE, Tenth Annual International Workshop*, 1997, pp. 262–266.

²P. E. Kiaditis, V. M. Bright, K. F. Harsh, and Y. C. Lee, 12th IEEE International Conference, 1999, pp. 570–575.

³L. N. Tsai, G. R. Shen, Y. T. Cheng, and W. S. Hsu, *The 54th Electronic Components and Technology Conference*, June 2004, pp. 472–476.

⁴G. R. Shen, L. N. Tsai, Y. T. Cheng, T. K. Lin, and W. S. Hsu, *IEEE Conference on Nanotechnology*, München, Germany, 2004, pp. 192–194.

⁵W. Zhao, C. Song, and P. E. Pehrsson, *J. Am. Chem. Soc.* 12418 (2002).

⁶C. S. Pan and W. S. Hsu, *J. Micromech. Microeng.* 7 (1997).

⁷X. H. Chen, F. Q. Cheng, S. L. Li, L. P. Zhou, and D. Y. Li, *Surf. Coat. Technol.* 274 (2002).

⁸K. S. Teh, Y. T. Cheng, and L. Lin, *12th International Conference on Solid State Sensors, Actuators and Microsystem*, Boston, 2003, pp. 1534–1537.

⁹G. R. Shen, Y. T. Cheng, and L. N. Tsai, *IEEE Trans. Nanotechnol.* 539 (2005).

¹⁰Y. Ando, X. Zhao, H. Shimoyama, G. Sakai, and K. Kaneto, *Inorg. Mater.* 77 (1999).